EO Signal Propagation in a Simulated Underwater Turbulence Environment

Weilin Hou
Naval Research Laboratory
Hydro Optics, Sensors and System Section
Stennis Space Center, MS, USA

Silvia Matt
National Research Council Research Associate
Stennis Space Center, MS, USA

Abstract— **Underwater electro-optical, or EO, transmission is a function of medium properties and constituents within. While the majority of the research focus has been on the constituents, especially the particulate forms, recent research indicates that under certain conditions, the apparent signal degradation could also be caused by variations of the index of refraction associated with temperature and salinity microstructure in oceans and lakes. These would inherently affect optical signal transmission underwater, which is important to both civilian and military applications involving search and rescue, intelligence, surveillance and reconnaissance applications, as well as optical communications.**

To study the effect of optical turbulence and to mitigate its impacts, a controlled environment allowing various intensities of turbulent mixing is a critical asset. Numerical experiments as well as measurements have been carried out in such a simulated environment, in order to understand mixing setup time, development and dissipation rates. The domain is modeled after a large Rayleigh-Bénard convective tank with a length, width and depth dimension of 5, 0.5 and 0.5m, respectively. The convective mixing is realized by using heating and cooling plates at the bottom and top of the tank at given temperature differences. The computational fluid dynamics model is implemented with large eddy simulation approximation. Dissipation rates from model and measurements are compared and suggest fully developed turbulence has been achieved by this setup. Optical signal transmission under these conditions are also examined, through image degradation using image quality metric, and phase screen models from corresponding power spectrum. The integrated temperature variation along the transmission path is compared to generated phase screens, along with discussions on reducing uncertainties in estimation of key parameters.

Keywords-component; controlled turbulence; simulation; Rayleigh-Bénard tank; phase screen; underwater; turbulence; optical scattering

I. INTRODUCTION

Recent research on underwater vision and optical, as well as acoustical signal propagation suggests better understanding is needed to quantify or mitigate the influence of underwater optical turbulence [1-5]. By its definition, turbulence is chaotic in nature, where statistical approach has been the only effective tool in quantifying related processes, along with idealized conditions and assumptions. Observations have been made both in lab and field, along with ancillary measurements, in order to have a reasonable estimate of the processes involved. The majority of the turbulence research has been carried out in the atmosphere, for studies related to weather events in general. Specific to optical signal transmission, the efforts are largely stemmed from the need to acquire better astronomical images of distant stars, which prompted the seminal paper by Fried[6], that the seeing is dependent of optical turbulence intensity, where it can be represented by the Fried seeing parameter r_0. If the wavelength of light passing through the system is λ, then the optical transfer function, OTF, or modulation transfer function when only amplitude is involved, is

$$H(\Psi) = \exp\left[-3.44\left(\frac{\lambda\Psi}{r_0}\right)^{\frac{5}{3}}\right] \quad (1)$$

here Ψ is the spatial frequency in cycles per radian, The exponential term in the OTF is essentially the structure function of the phase variation, due to the index of refraction change caused by the temperature variation in the atmosphere. This relates back to the basic statistical imaging principle, where the interference between two field points forms the image that describes the spatial coherency. This is known as the Van Cittert-Zernike theorem [7, 8], and essentially the two dimensional view of the famous Young's interference experiment. The spatial perturbations during the wave propagation alter the imaging outcome at the pupil plane, by altering the interference fringe patterns. Due to the nature of turbulent flow in the atmosphere, where the motion follows lateral wind directions and density structures, a layered approach can be used for most astronomy, as well as reconnaissance imaging needs. However, this is not the case for the most oceanic turbulence study, unless vertical optical transmissions through strong horizontal layers are involved.

A few assumptions have to be made to properly describe the seemingly random, chaotic process loosely termed turbulence. Even from the observations from early days, like those of Da Vinci and his water swirl drawing, we understand that turbulence relates to the way energy dissipates across various spatial scales. Kolmogorov's classical theory of turbulence is often used, where fully developed isotropic homogeneous turbulence conditions are assumed, and the energy spectrum follows the -5/3 law in the inertial sub-range, based on dimensional analysis. This is the condition for which

This project was funded by ONR/NRL Program Element 62782N.

the above equation was derived, and we can clearly see the trademark signature in the equation. While sounding somewhat contradictory, a wide-sense stationary condition has to be reached, in a statistical sense over temporal (stable) and spatial scales (isotropic), in order to describe the kinetic energy dissipation, as well as other scalar quantities.

Until recently, the standing view about the source of underwater electro-optical (EO) imaging degradation has been the scattering by the medium itself and the constituents within, namely particles of various origins and sizes. Recent research indicates that under certain conditions, the apparent degradation could also be caused by variations of the index of refraction associated with temperature and salinity micro-structures in oceans and lakes [1, 5, 9]. These would inherently affect optical signal transmissions underwater. Two of the key parameters commonly used to describe turbulence are directly related to the optical turbulence intensity, S_n, [1, 5], a coefficient directly related to the optical transfer function (OTF) of the turbulence impact (see Eq. 3 below), shown in the form below, including path radiance and particle scattering contributions:

$$\begin{aligned} OTF(\psi,r)_{total} &= OTF(\psi,r)_{path} OTF(\psi,r)_{par} OTF(\psi,r)_{tur} \\ &= \left(\frac{1}{1+D}\right)\exp\left[-cr + br\left(\frac{1-e^{-2\pi\theta_0\psi}}{2\pi\theta_0\psi}\right)\right]\exp\left(-S_n\psi^{5/3}r\right) \\ &= \left(\frac{1}{1+D}\right)\exp\left\{-\left[c - b\left(\frac{1-e^{-2\pi\theta_0\psi}}{2\pi\theta_0\psi}\right) + S_n\psi^{5/3}\right]r\right\} \end{aligned} \quad (2)$$

here θ_0 relates to the mean scattering angle, c and b are the beam attenuation and scattering coefficients respectively. r is the imaging range, and D relates to path radiance [3]. S_n contains parameters that are dependent on the structure function, which can be further expressed in terms of the turbulence dissipation rate of temperature, salinity and kinetic energy, assuming the Kolmogorov power spectrum type:

$$S_n \sim \chi\varepsilon^{-1/3} \quad (3)$$

where ε, χ represent the kinetic energy and temperature variance dissipation rates, respectively. These are the key parameters to be determined from numerical simulations, as well as measurements.

Only a simple case of a point source response to the imaging system needs to be examined, as all image formation can be treated as a convolution between a point source and system transfer function [1, 10]. For continuous wave front distortions, as a result of turbulence degradation satisfying Eq. 1, it has been shown that a Fourier transform pair links the phase fluctuation and corresponding power spectrum [7, 8]. One can then sample the power spectrum (in this case, temperature variance dissipation) to create phase screens, which represents layered distortions or integrated effects. The covariance approach will not be discussed in this initial effort.

To better understand turbulent microstructure, especially those associated with temperature and salinity variations in the underwater environment, it would be ideal if a repeatable, somewhat controllable environment can be implemented. This is the motivation of our Rayleigh-Bénard (RB) convective tank setup at the U.S. Naval Research Laboratory at the Stennis Space Center, MS. We will first discuss the setup and lab experiment, and numerical simulations, as our attempt to establish a controlled turbulence environment. This will be followed by observations on image quality degradation through the controlled environment, and related phase variations under different power distribution schemes associated with the controlled environment.

II. Simulation of Controlled Environment

A 5 by 0.5 by 0.5 m (L, H, W) plexiglass tank has been fitted with stainless steel plates, in order to control the surface and bottom temperature for generation and maintenance of convective mixing (Figure 1). This classical Rayleigh-Benard tank allows generation of optical turbulence at various intensities, shown by an example in Figure 2. The left side of the panel displays a turbulence-free image through filtered water over 5m in pathlength, under a beam attenuation value less than $0.1m^{-1}$ measured by an ac-9 (WETLabs). Without particle's presence, when the optical turbulence intensity increases due to an increase of the temperature gradient between the plates, one can see the severe degradation of imaging resolution by examining the resolution chart shown by the frame on the right of Figure 2, which is in line with results of Eq.2. Note that in the foreground of the image is a partial image of an Acoustical Doppler Velocimeter (ADV), made by Nortek, which can also been seen in Figure 1 (left). These are used to measure the small-scale velocities in the tank during the experiment, along with fast conductivity and temperature probe (CT) from PME, and three smaller profiling ADVs, Vectrino (Fig.1, right), also from Nortek. For initial examination, seeding necessary for ADV measurements are added to the tank after optical measurement using the same temperature gradient setup, to ensure only turbulence effects on optical signal transmission are in place. This does not affect the circulation pattern, once the gradient is set. This is confirmed by numerical simulations to be discussed below. These measurements are necessary to help model setup, as well as validation.

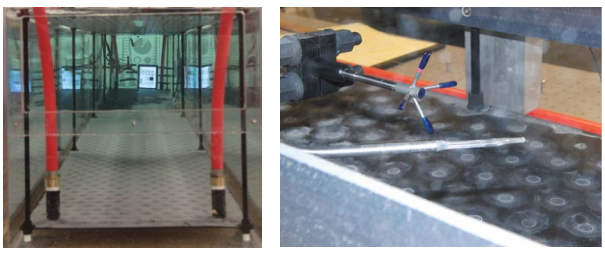

Figure 1. Rayleigh-Bénard convective tank setup at the U.S. Naval Research Laboratory, Stennis Space Center. Different temperature

gradients are implemented by two stainless steel plates on top and bottom. Left panel: along tank view of target through filtered water with ADV embedded; Right panel: close-up view of CT and ADV setup (see text for details).

The governing equation of any fluid is straight-forward Navier-Stokes equation, shown below for incompressible fluid, in the absence of external forcing [11]:

$$\frac{\partial \mathrm{V}}{\partial t} + \mathrm{V}\boldsymbol{\nabla}\mathrm{V} = -\frac{\boldsymbol{\nabla p}}{\boldsymbol{\rho}} + \boldsymbol{\nu}\boldsymbol{\nabla^2}\mathrm{V} \qquad (4)$$

where $\boldsymbol{\nu}$ is the kinematic viscosity. In most cases it is not possible to arrive at an analytical solution to recover the flow field. Numerical solution using high speed computers has proven to be an effective tool. The domain of interest can be subdivided into grid points, at which a solution can be obtained by discretizing the governing equations (including Eq. 4, in addition to continuity and energy) in space and time, for a given set of boundary and initial conditions.

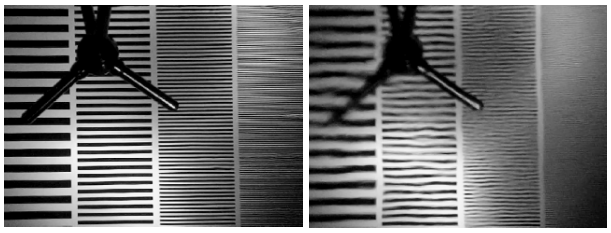

Figure 2. Sample images of impact of optical turbulence over 5m pathlength in water, viewing resolution chart and ADV in the foreground. Left: turbulence free; Right: strong optical turbulence.

However, sacrifices have to be made due to the cost of computation, especially at fine spatial and temporal resolution, which is necessary for microstructure studies. Scale discrepancies between different physical processes demand approximations to be made, as a compromise, even with powerful supercomputers. For example, the optical wave field phenomenon requires sub-picosecond resolution to be fully resolved, which is not possible in practical underwater applications at the moment. Even at this rate, it is not sufficient to include the spatial resolution requirement comparable to the wavelength of light (which is sub-micron), in order to study processes involving wave field interactions for typical visible wavelength. Another example can be found in our computational fluid dynamics (CFD) approach, where the scales of turbulent flow cover several orders of spatial magnitude that can be prohibitively expensive, to fully solve using direct numerical simulation (DNS) of Eq. 4. Traditionally, several parameterizations have been developed to model the sub-grid scale turbulence processes, including Reynolds-averaged Navier-Stokes (RANS), and large eddy simulation (LES). LES is essentially a low-pass filtering approach, where larger scales are resolved while the finer scales are modeled. LES explicitly resolves the larger eddies in the flow, and models processes smaller than the grid spacing. This improves the physical representation of the turbulent field, and is adopted for our work. An open-source CFD package, OpenFOAM, is used, with traditional Smagorinsky model as a sub-grid scale model. Two resolutions have been investigated, on at 1cm (x,y,z) and one at 2.5 mm (for horizontal x, y) and 5mm (for vertical, z). These are equivalent of 1.25 and 20 million grid points, respectively. The temperature distribution of simulation under fully-developed (time=1050s), strong turbulence conditions is shown in Figure 3. The index of refraction (IOR) in the tank is calculated based on relationship to the temperature fields [12].

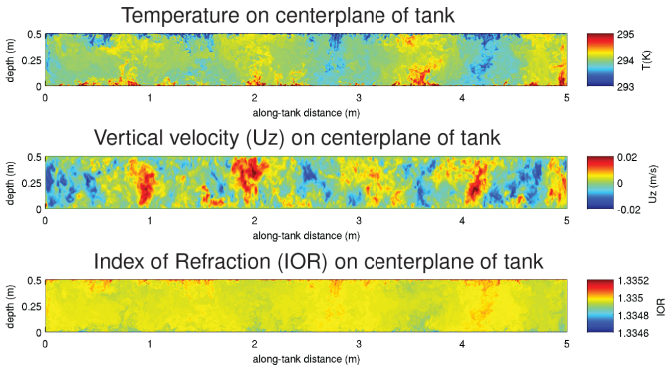

Figure 3. LES simulation temperature (in Kelvin), vertical velocity and IOR in the Rayleigh-Bénard convective tank under strong turbulence, when fully developed (see text for details).

One may notice that several larger scale convective cells (~1.5m) are present in the above simulation output, which is confirmed by visual observations, as well as temperature measurements.

One of the challenges of quantifying the turbulence intensities, and comparing to the measurements, is the fact that it is challenging to accurately capture the temporal and spatial variability represented by the simulation with corresponding measurements. At least two factors are in play here. The first is the initiation and maintenance of the statistically stable environment. This can be seen from the variations shown in Figure 4. One may notice that after initial setup, the variance of both temperature and velocity begins to reduce to a stable level, with smaller oscillations likely resulting from larger cell movements within the tank, as well as naturally occurring intensity fluctuations local to the sensors.

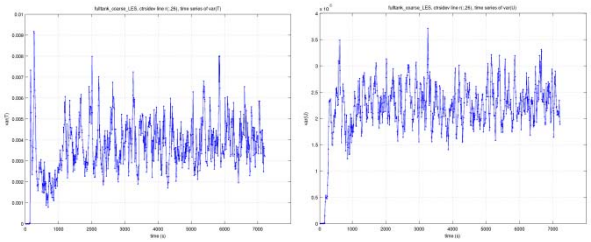

Figure 4. Times series of temperature and vertical velocity variance, taken from the center line of the tank, using cm-resolution run.

Obviously, this poses a challenge in quantifying the turbulent dissipation rates we discussed earlier, both of

temperature variance and kinetic energy. The energy spectra from tank measurements, and model output are shown in Figure 5. We see that they all exhibit a well resolved inertial subrange, where the signature energy spectrum slope of -5/3 is marked. This is a clear confirmation that we have achieved the initial goal of setting up a controlled turbulence environment.

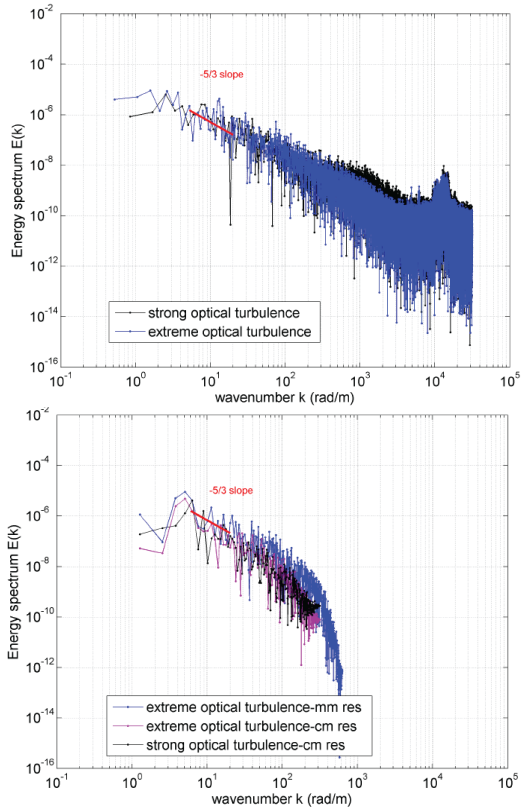

Figure 5. Kinetic energy spectra from lab measurement for both strong and extreme turbulence case (top), compared to LES mode output (bottom).

We also notice from Figure 5 the differences between mm- and cm-resolution output, and potential issues associated with Taylor's frozen turbulence hypothesis. More in depth understanding and discussion is needed, along with more case studies, which will be discussed in a separate paper. We now turn our attention to EO transmission in this controlled environment.

III. IMAGING TRHOUGH CONTROLLED TURBULENCE

It has been modeled and validated in previous studies [1, 5, 13], that optical turbulence does degrade image quality, as also seen by our tank experiment results, shown in Figure 6. Cases of transmission through non-turbulence, strong and extreme turbulence are displayed. It can be seen, along with Figure 2, that optical turbulence degradation is frequency dependent, as predicted by Eq.2.

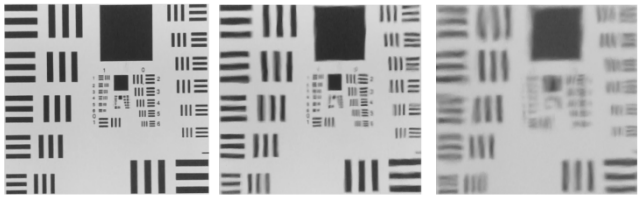

Figure 6. Image transmission through non-, strong- and extreme-optical turbulence from RB tank at NRL SSC.

To examine the variation of image degradation, a structure similarity index metric (SSIM) is used, which has been shown to be very sensitive to the image quality variations with known pristine reference [14], including time-varying influences such as turbulence impacts. A time series of SSIM from our tank experiment is shown in Figure 7. We notice the reduced variance, which indirectly confirms our conclusion of a controlled environment of the previous section. It can be seen that such metric does follow the trend of the turbulence intensity reasonably well, at least for the two cases of strong and extreme conditions we tested. This further suggests that it could be used as a proxy for OTF, given known optical conditions associated with Eq. 2.

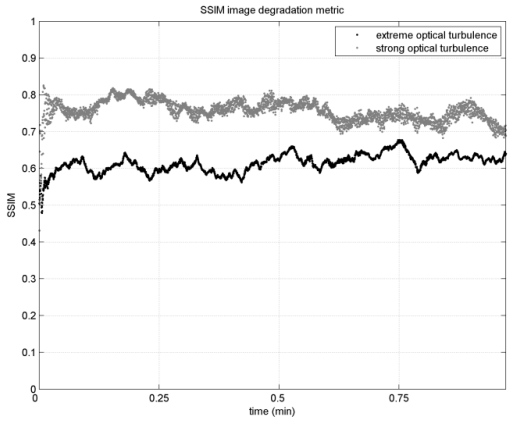

Figure 7. Time series of image degradation during our lab experiment, under strong and extreme turbulence case.

In atmospheric studies, where turbulence often affects astronomical observations, an effective approach is based on statistical method using layered medium, with diffraction propagation between layers. The phase variation of each layer can be easily obtained from the power spectrum of the phase, in 3d case, this is typically [7]

$$\Phi(k) = 0.033 C_n^2 |k|^{-11/3} \tag{5}$$

with C_n^2 denotes turbulence intensity; or in practice, such as in our test case shown, modified von Karman spectrum is more appropriate, which eliminates the issues at very high and low spatial frequencies

$$\Phi^V(k) = 0.033 \frac{C_n^2}{(k^2+k_0^2)^{11/6}} \exp\left(-\frac{k^2}{k_m^2}\right) \tag{6}$$

where k_m and k_0 corresponds to inner and outer scales.

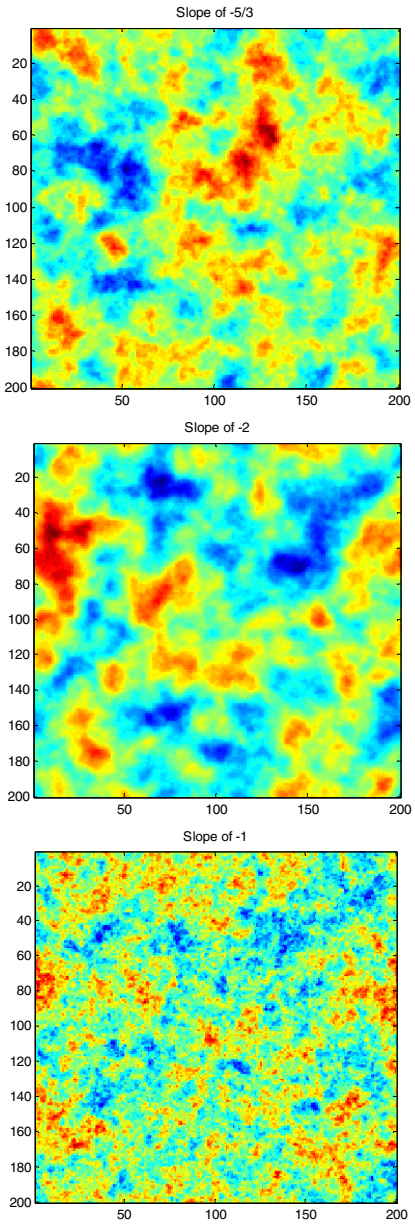

Figure 8. Phase screens generated using Fourier transfer based on spectrum model of different spectral slopes. Top: Kolmogorov type with -5/3 slope; Middle: steep reduction with a slope of -2, resemble small scale processes; Bottom: gradual decrease of energy at a slope of -1. All based on von Karman shown in Eq.6.

Applying formulas derived for underwater conditions [1], phase screens using spectral method are generated, following Lane et al [15]. Typical underwater conditions corresponding to natural conditions are used, with inner and out scales set at 0.001 and 1.5m to reflect the tank conditions. The results are shown in Figure 8. As mentioned earlier, it is interesting to observe the uncertainty in the slope of the energy spectrum, which can span a significant range, even in a well-established, fully developed turbulence environment (Fig.5). Coupled with the progress and time taken to reach a stationary environment, it is reasonable to assume that different spectral slopes exist, and worth the investigation of impacts under such variable conditions. This is the reason behind the middle and lower panels of Figure 8, where the influence of spectral slope is shown in the form of a typical phase screen, compared side by side to the traditional Kolmogorov one shown in the top panel of Figure 8. Strong contrast can be seen, especially between fast energy reduction (middle) and slow diffusion (bottom). Notice that the color is added to contrast variation and only the pattern variability should be taken into considerations.

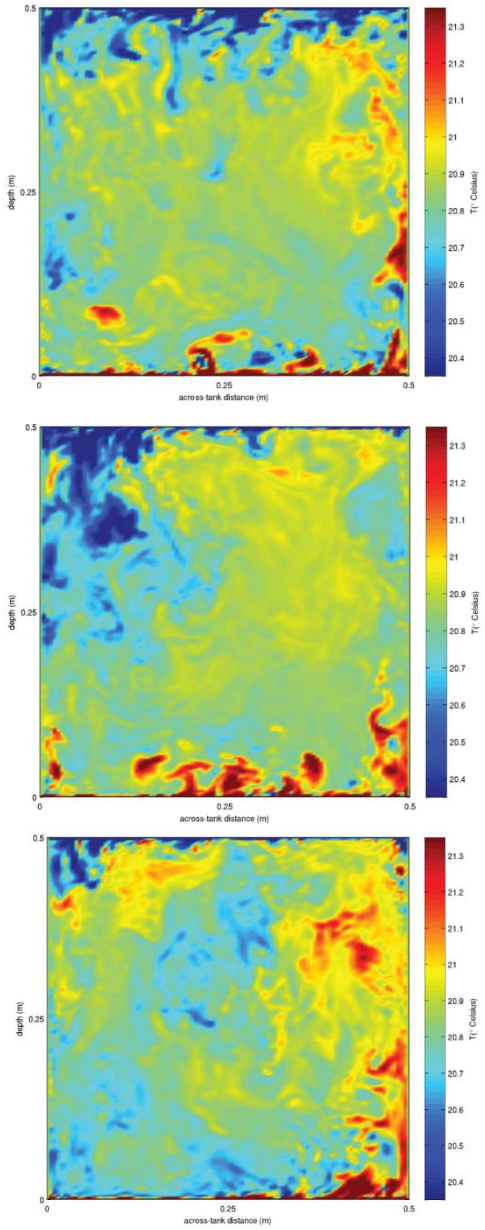

Figure 9. Cross-sectional view of temperature variations at the center of the tank under a fully developed turbulence condition, taken from cm-resolution numerical results at t=850s, 875, and 950s respectively, from top to bottom.

To provide a comparison of spatial variability across the tank cross-section, the temperature profiles from mm-resolution LES output are shown in Figure 9, at time=850, 875 and 950s. One can clearly see the large to small scale vortices. Notice that the phase screen in Fig. 8 is representative of the center of the tank conditions, while the cross-sectional plots shown in Fig. 9 depict a much larger area. Visual observation suggest that the top two panels of Fig. 8 are closer to reality than the last panel, when Fig. 9 is used as the benchmark.

IV. SUMMARY

Efforts have been made to create a controlled environment, under which stochastic processes like ocean turbulent mixing can be studied. This paper presents a first attempt to study the impact of optical turbulence on EO signal transmission underwater under such conditions. A LES numerical model is used to simulate and monitor the mixing process. Measurements using ADVs were taken to validate numerical output. Comparisons presented indicate a successful match has been found between the simulation and measurements, although further exercise is pending, to obtain repeatable outcome at various grid sizes and turbulence intensities. Optical transmission through the RB tank are also recorded. Degradation by turbulence is related to image quality metric and may be used as a proxy for turbulence intensity estimation. Phase screens based on the von Karman spectrum are shown, which are in line with variations of the numerical tank. Uncertainty estimation of the power spectrum slope has been discussed, and more efforts are necessary in order to increase confidence in the estimation, and establish direct comparison to a complex phase screen model involving scattering and absorption.

ACKNOWLEDGMENT

This research was supported by ONR program element 62782N.

REFERENCES

1 Hou, W.: 'A simple underwater imaging model', Opt. Lett., 2009, 34, (17), pp. 2688-2690

2 Hou, W., Jarosz, E., Woods, S., Goode, W., and Weidemann, A.: 'Impacts of underwater turbulence on acoustical and optical signals and their linkage', Opt. Express, 2013, 21, (4), pp. 4367-4375

3 Hou, W.: 'Ocean Sensing and Monitoring: Optics and Other Methods' (SPIE Press, 2013.)

4 Hou, W., Woods, S., Goode, W., Jarosz, E., and Weidemann, A.: 'Impacts of optical turbulence on underwater imaging'. Proc. SPIE Defense and Security, Orlando, FL, 2011

5 Hou, W., Woods, S., Jarosz, E., Goode, W., and Weidemann, A.: 'Optical turbulence on underwater image degradation in natural environments', Appl. Opt., 2012, 51, (14), pp. 2678-2686

6 Fried, D.L.: 'Optical resolution through a randomly inhomogeneous medium for a very long and very short exposures', J. Opt. Soc. Am., 1966, 56, pp. 1372-1379

7 Roggemann, M.C., and Welsh, B.M.: 'Imaging through turbulence' (CRC Press, 1996. 1996)

8 Goodman, J.W.: 'Statistical Optics' (John Wiley & Sons, 1985. 1985)

9 Gilbert, G.D., and Honey, R.C.: 'Optical turbulence in the sea', in Editor (Ed.)^(Eds.): 'Book Optical turbulence in the sea' (SPIE, 1972, edn.), pp. 49-55

10 Hou, W., Lee, Z., and Weidemann, A.: 'Why does the Secchi disk disappear? An imaging perspective', Opt. Express, 2007, 15, (6), pp. 2791-2802

11 Tennekes, H., and Lumley, J.L.: 'A First Course in Turbulence' (Pe Men Book Company, 1972. 1972)

12 Quan, X., and Fry, E.S.: 'Empirical equation for the index of refraction of seawater', Applied Optics, 1995, 34, (18), pp. 3477-3480

13 Nootz, G., Hou, W., Dalgleish, F.R., and Rhodes, W.T.: 'Determination of flow orientation of an optically active turbulent field by means of a single beam', Optics letters, 2013, 38, (13), pp. 2185-2187

14 Wang, Z., Bovik, A.C., Sheikh, H.R., and Simoncelli, E.P.: 'Image quality assessment: from error visibility to structural similarity', IEEE Trans. on Image Proc., 2004, 13, (4), pp. 600-612

15 Lane, R.G., Glindemann, A., and Dainty, J.C.: 'Simulation of a Kolmogorov phase screen', Waves in Random Media, 1992, 2, (3), pp. 209-224